Three-Dimensional Structure of Tyrosine Phenol-lyase[†,‡]

Alfred A. Antson,[§,∥,⊥] Tatyana V. Demidkina,[#] Paul Gollnick,[○] Zbigniew Dauter,[∥] Robert L. Von Tersch,[×] John Long,[○] Sergey N. Berezhnoy,[#] Robert S. Phillips,[*,×] Emil H. Harutyunyan,[§] and Keith S. Wilson[∥]

Shubnikov Institute of Crystallography, Russian Academy of Sciences, Leninsky pr. 59, Moscow 117333, Russia, European Molecular Biology Laboratory (EMBL), c/o DESY, Notkestrasse 85, D-2000 Hamburg 52, Germany, Engelhardt Institute of Molecular Biology, Russian Academy of Sciences, 32 Vavilov Street, Moscow 117984, Russia, Departments of Chemistry and Biochemistry, University of Georgia, Athens, Georgia 30602, and Department of Biological Sciences, Cooke Hall, State University of New York at Buffalo, Buffalo, New York 14260

Received September 29, 1992; Revised Manuscript Received January 22, 1993

ABSTRACT: Tyrosine phenol-lyase (EC 4.1.99.2) from *Citrobacter freundii* has been cloned and the primary sequence deduced from the DNA sequence. From the BrCN digest of the $NaBH_4$-reduced holoenzyme, five peptides were purified and sequenced. The amino acid sequences of the peptides agreed with the corresponding parts of the tyrosine phenol-lyase sequence obtained from the gene structure. K257 is the pyridoxal 5′-phosphate binding residue. Assisted by the sequence data, the crystal structure of apotyrosine phenol-lyase, a pyridoxal 5′-phosphate-dependent enzyme, has been refined to an *R*-factor of 16.2% at 2.3-Å resolution using synchrotron radiation diffraction data. The tetrameric molecule has 222 symmetry, with one of the axes coincident with the crystallographic 2-fold symmetry axis of the crystal which belongs to the space group $P2_12_12$ with $a = 76.0$ Å, $b = 138.3$ Å, and $c = 93.5$ Å. Each subunit comprises 14 α-helices and 16 β-strands, which fold into a small and a large domain. The coenzyme-binding lysine residue is located at the interface between the large and small domains of one subunit and the large domain of a crystallographically related subunit. The fold of the large, pyridoxal 5′-phosphate binding domain and the location of the active site are similar to that found in aminotransferases. Most of the residues which participate in binding of pyridoxal 5′-phosphate in aminotransferases are conserved in the structure of tyrosine phenol-lyase. Two dimers of tyrosine phenol-lyase, each of which has a domain architecture similar to that found in aspartate aminotransferases, are bound together through a hydrophobic cluster in the center of the molecule and intertwined N-terminal arms.

Pyridoxal 5′-phosphate- (PLP-)[1] containing enzymes perform a variety of reactions in the metabolic pathways of amino acids, including transamination, β- and γ-elimination and replacement, decarboxylation, and racemization. Tyrosine phenol-lyase (TPL; EC 4.1.99.2) is a PLP-dependent enzyme that catalyzes the β-elimination of L-tyrosine to give phenol and ammonium pyruvate (Kumagai et al., 1970a,b). The molecule of TPL consists of four chemically identical subunits (Kazakov et al., 1987), each with molecular mass about 50 kDa, and binds 4 mol of PLP per tetramer. This enzyme is found primarily in enterobacteria (Enei et al., 1972), although it has been reported to occur in some arthropods (Duffey & Blum, 1977; Duffey et al., 1977).

X-ray analyses of PLP-dependent enzymes from several different classes are presently underway. X-ray crystallographic studies have been carried out on a number of aminotransferases [full references are given in Fukui et al. (1991)] from different sources, beginning with the determination of the three-dimensional structure of chicken mitochondrial (Ford et al., 1980), chicken cytosolic (Borisov et al., 1980; Harutyunyan et al., 1982), and pig cytosolic (Arnone et al., 1985) aspartate aminotransferase (AspAT). Each active site of the α_2 molecule of AspAT is composed of residues from both the large and small domains of one subunit and the large domain of the other subunit. The active site residues are invariant in AspAT from different sources (Kondo et al., 1987), including bacterial and mammalian enzymes. In the three-dimensional structure of the $\alpha_2\beta_2$ molecule of *Salmonella typhimurium* tryptophan synthase (Hyde et al., 1988), in which the β_2-dimer catalyzes the β-replacement reaction, the active sites of the two β subunits are quite distant, and residues from one β subunit do not contribute to the active site of the other. Determination of the three-dimensional structures of β-eliminating lyases is in progress: crystals of tyrosine phenol-lyase (TPL) (Demidkina et al., 1988) and a related enzyme, tryptophan indole-lyase (tryptophanase, TRPase; EC 4.1.99.1) (Kawata et al., 1991), suitable for X-ray analysis have been obtained.

Early difficulties in the solution of the three-dimensional structure of TPL were mainly due to instability of the crystals to X-irradiation and to the absence of primary sequence

[†] A.A.A. thanks the EMBL, Hamburg, for a fellowship supporting this work. This work was partially supported by a grant from the National Institutes of Health (GM 42588) to R.S.P.

[‡] Crystallographic coordinates have been deposited in the Brookhaven Protein Data Bank under the filename 1TPL. The nucleotide sequence has been deposited in GenBank under Accession Number L10821.

[§] Shubnikov Institute of Crystallography.

[∥] European Molecular Biology Laboratory.

[⊥] Present address: Department of Chemistry, University of York, Heslington, York Y01 5DD, England.

[#] Engelhardt Institute of Molecular Biology.

[○] State University of New York at Buffalo.

[×] University of Georgia.

[1] Abbreviations: PLP, pyridoxal 5′-phosphate; TPL, tyrosine phenol-lyase (EC 4.1.99.2); AspAT, aspartate aminotransferase; TRPase, tryptophan indole-lyase (tryptophanase) (EC 4.1.99.1).

0006-2960/93/0432-4195$04.00/0

```
   1 TGTAAATTACCCCAGTAATTGGCGGGAAGTCCAGATGTAAATAACATGAAATAAGGGATT
  61 AGCAGGTTTCGGAATAAATAGAAATCCTCTCTATCCCAATAAACATAGTATTATTCACCG
 121 TATAAATTCATTCCTGTCCCATCCTCCTGATACCTGCCATTTCCAGAAAATAACGCCCAT
 181 GTGTATCAGGCCAAAAATGAGATCTAACTCACTGAAGCAAATAGCAAACTCTGAAACAAC
 241 GCCGTTTTGTACACTTTGCTTTACACTTTTAGTGATGTGAATCACAAATATAAATCCGTG
 301 AAGTGATCCGACTCTCACAAAATGGGGTGTACTCATTCAGCAATACAGTATGAGCACAGA
 361 CTGGAAAGTTAAGTTTTCAGTATTTCCCCTCTCCACGGGGGCAcCATCGCAAATGGCAAA
 421 TCAACACGCAAAAAAAAACTTGTTGAATATGAACGGGTAAAAAAATGACGTGTGATTTGC
 481 ATCACCTACATTTACAGCTTTTTAAATTATTGCCAGTGATTAATGTTGACTAGGCTATTT
 541 CCATAATCAATTAAATCTTGCATAGTGCCTCCACATTATTTCTCCCCCTGACTCAGGAGG
 601 CGAATAGTTATATTTCATCAGACTTTATTGATGAACCAGGTATGCTTTACTTCACATTAA

 661 TACGTACATGACCACTGTTACTGGAGAAACAAAATGAATTATCCGGCAGAACCCTTCCGT
                                   MetAsn TyrProAlaGlu ProPheArg

 721 ATTAAAAGCGTTGAAACTGTATCTATGATCCCGCGTGATGAACGCCTTAAGAAAATGCAG
     IleLysSerValGluThrValSerMetIleProArgAspGluArgLeuLysLysMetGln

 781 GAAGCGGGATACAATACTTTCCTGTTAAATTCGAAAGATATTTATATTGACCTGCTGACA
     GluAlaGlyTyrAsnThrPheLeuLeuAsnSerLysAspIleTyrIleAspLeuLeuThr

 841 GACAGTGGCACTAACGCAATGAGCGACAAGCAGTGGGCCGGCATGATGATGGGTGATGAA
     AspSerGlyThrAsnAlaMetSerAspLysGlnTrpAlaGlyMetMetMetGlyAspGlu

 901 GCCTACGCGGGCAGCGAAAACTTCTATCATCTGGAAAGAACCGTGCAGGAACTGTTTGGC
     AlaTyrAlaGlySerGluAsnPheTyrHisLeuGluArgThrValGlnGluLeuPheGly

 961 TTTAAACATATTGTTCCTACTCACCAGGGGCGCGGCGCAGAAAACCTGTTATCGCAGCTG
     PheLysHisIleValProThrHisGlnGlyArgGlyAlaGluAsnLeuLeuSerGlnLeu

1021 GCAATTAAACCGGGGCAATATGTTGCCGGGAATATGTATTTCACTACTACCCGTTATCAC
     AlaIleLysProGlyGlnTyrValAlaGlyAsnMetTyrPheThrThrThrArgTyrHis

1081 CAGGAAAAAAAATGGTGCGGTGTTTGTCGATATCGTTCGTGACGAAGCGCACGATGCCGGT
     GlnGluLysAsnGlyAlaValPheValAspIleValArgAspGluAlaHisAspAlaGly

1141 CTGAATATTGCTTTTAAAGGTGATATCGATCTTAAAAAATTACAAAAACTGATTGATGAA
     LeuAsnIleAlaPheLysGlyAspIleAspLeuLysLysLeuGlnLysLeuIleAspGlu

1201 AAAGGCGCCGAGAATATTGCCTATATTTGCCTGGCAGTCACGGTTAACCTCGCAGGCGGG
     LysGlyAlaGluAsnIleAlaTyrIleCysLeuAlaValThrValAsnLeuAlaGlyGly

1261 CAGCCGGTTTCCATGGCTAACATGCGCGCGGTGCGTGAACTGACTGCAGCACATGGCATT
     GlnProValSerMetAlaAsnMetArgAlaValArgGluLeuThrAlaAlaHisGlyIle

1321 AAAGTGTTCTACGACGCTACCCGCTGCGTAGAAAACGCCTACTTTATCAAAGAGCAAGAG
     LysValPheTyrAspAlaThrArgCysValGluAsnAlaTyrPheIleLysGluGlnGlu

1381 CAGGGCTTTGAGAACAAGAGCATCGCAGAGATCGTGCATGAGATGTTCAGCTACGCCGAC
     GlnGlyPheGluAsnLysSerIleAlaGluIleValHisGluMetPheSerTyrAlaAsp
                                *
1441 GGTTGTACCATGAGTGGTAAAAAAGACTGTCTGGTGAATATCGGCGGCTTCCTGTGCATG
     GlyCysThrMetSerGlyLysLysAspCysLeuValAsnIleGlyGlyPheLeuCysMet

1501 AACGATGACGAAATGTTCTCTTCTGCCAAAGAGTTAGTCGTTGTCTACGAAGGCATGCCA
     AsnAspAspGluMetPheSerSerAlaLysGluLeuValValValTyrGluGlyMetPro

1561 TCTTACGGCGGCCTGGCCGGACGCGACATGGAAGCCATGGCGATTGGTCTGCGCGAAGCC
     SerTyrGlyGlyLeuAlaGlyArgAspMetGluAlaMetAlaIleGlyLeuArgGluAla

1621 ATGCAGTATGAGTACATCGAGCACCGCGTGAAGCAGGTTCGCTATCTGGGCGACAAGCTG
     MetGlnTyrGluTyrIleGluHisArgValLysGlnValArgTyrLeuGlyAspLysLeu

1681 AAAGCCGCTGGTGTACCGATTGTTGAACCGGTGGGCGGTCATGCGGTATTCCTCGATGCG
     LysAlaAlaGlyValProIleValGluProValGlyGlyHisAlaValPheLeuAspAla

1741 CGTCCGTTCTGTGAGCATCTGACGCAGGACGAGTTCCCGGCGCAAAGCCTGGCTGCCAGT
     ArgProPheCysGluHisLeuThrGlnAspGluPheProAlaGlnSerLeuAlaAlaSer

1801 ATCTATGTGGAAACCGGCGTACGTAGTATGGAGCGCGGAATTATCTCTGCGGGCCGTAAT
     IleTyrValGluThrGlyValArgSerMetGluArgGlyIleIleSerAlaGlyArgAsn

1861 AACGTGACTGGTGAACACCACAGGCCGAAACTGGAAACCGTGCGTCTGACTATTCCACGC
     AsnValThrGlyGluHisHisArgProLysLeuGluThrValArgLeuThrIleProArg
```

```
1921 CGCGTTTATACTTACGCGCATATGGATGTAGTGGCTGACGGTATTATTAAACTTTACCAG
     ArgValTyrThrTyrAlaHisMetAspValValAlaAspGlyIleIleLysLeuTyrGln

1981 CACAAAGAAGATATTCGCGGGCTGAAGTTTATTTACGAGCCGAAGCAGCTCCGTTTCTTT
     HisLysGluAspIleArgGlyLeuLysPheIleTyrGluProLysGlnLeuArgPhePhe

2041 ACTGCACGCTTTGACTATATCTAAATAATAATTATGGCCCCATCTCAGGATCGGTCCTTT
     ThrAlaArgPheAspTyrIleEnd

2101 TTTGATTTCTTTTCCATGAACAGGAAGTCCTTT
```

FIGURE 1: Nucleotide sequence of the *tpl* gene from *C. freundii* and the deduced amino acid sequence. Amino acid sequences determined from N-terminal Edman analysis and isolated peptides are underlined.

information. The data collection problem has been solved by using synchrotron radiation at short wavelength. The determination of the primary sequence of TPL from *Citrobacter freundii* greatly accelerated the progress of three-dimensional model building. The course of the polypeptide chain and the subunit topology of TPL were described previously on the basis of a preliminary atomic model of the enzyme (Antson et al., 1992). It was shown that the domain architecture in the TPL dimer formed by the crystallographically related subunits and the topology of the large domain are analogous to those in the α_2 molecule of aspartate aminotransferase (AspAT) and quite different from those found in the β_2-dimer of the $\alpha_2\beta_2$ molecule of tryptophan synthase. Recently, phases were improved to allow the construction of a model sufficiently good for least-squares refinement to be carried out. The three-dimensional structure of the apoenzyme of TPL is reported here at a resolution of 2.3 Å, together with the determination of the DNA sequence of the *tpl* gene from *C. freundii*, deduction of the primary amino acid sequence, and location of the PLP-binding lysine.

MATERIALS AND METHODS

Purification of TPL from *C. freundii* (ATCC 29063) and *Citrobacter intermedius* was achieved by a modification of published procedures (Carman & Levin, 1977; Demidkina, 1984), with the introduction of hydrophobic chromatography on Octyl-Sepharose CL-4B as the key step (Phillips et al., 1987). The purified enzyme was a single band on SDS–polyacrylamide gels with an approximate molecular mass of 46 kDa (data not shown). The sequence of the first 17 amino acids from the amino terminus of *C. freundii* TPL was determined by automated Edman degradation, and the sequence obtained is indicated by underlining in the complete sequence in Figure 1.

Cloning the tpl gene from *C. freundii* was accomplished using a genomic library constructed in λZAP II (Stratagene). The library was packaged into λ using Gigapack (Stratagene) and then plated on BB4 *Escherichia coli* host cells. The library was screened by plaque hybridization (Benton & Davis, 1977) using a degenerate oligonucleotide probe (oligo 850) for the *tpl* gene on the basis of the N-terminal amino acid sequence (Figure 1) that had been ^{32}P-end-labeled using polynucleotide kinase and [γ-^{32}P]ATP (Sambrook et al., 1989). Five positive clones were obtained, containing inserts ranging from 600 to 6000 kb. The pBlueScript plasmid from each was excised in vivo using R408 helper phage and *E. coli* XL1 Blue (Stratagene). The presence of the start of the *tpl* coding region on each plasmid was confirmed by DNA sequencing using oligo 850 as the primer.

Extracts from *E. coli* SVS370 [W3110 *bgl*R551 Δ(*trp*EA)2 *tna*270::*Tn*5] transformed with each plasmid were tested for TPL activity using an assay based on cleavage of *S*-(*o*-nitrophenyl)-L-cysteine (Phillips, 1987). Extracts from cells containing pTPL6B and pTPL2A contained significant TPL activity. These plasmids contained 4- and 6-kbp inserts, respectively. Extracts from cells transformed with pTPL2A consistently contained higher levels of TPL activity than those from pTPL6B. We therefore chose to characterize the *tpl* gene from pTPL2A.

Table I: Statistics of the Synchrotron Diffraction Data

resolution ranges	$\langle I \rangle$	$\langle I/\sigma(I) \rangle$	redundancy	R_{merge}	completeness[a] %	completeness[a] % > 3σ
15.0–6.61	2834	20.2	4.4	0.031	92.4	91.3
6.61–4.92	1567	15.1	5.3	0.041	98.5	95.9
4.92–4.09	1954	13.7	5.4	0.046	98.4	96.5
4.09–3.57	1393	12.0	5.1	0.053	98.3	95.1
3.57–3.22	649	12.7	3.7	0.056	98.3	92.5
3.22–2.95	415	10.3	3.7	0.076	98.8	88.2
2.95–2.74	253	6.9	3.7	0.109	98.4	81.8
2.74–2.56	175	5.1	3.7	0.146	98.4	75.7
2.56–2.42	128	3.9	3.6	0.190	98.0	65.3
2.42–2.30	104	3.3	3.6	0.225	97.8	59.0
total	772	9.3	4.1	0.058	97.8	80.8

[a] Two values for the completeness of the data with reference to the theoretically possible number are given. The first is the percentage of data measured and the second the percentage greater than 3σ.

Mapping the tpl Gene within the Cloned Fragment. The *tpl* gene within the cloned fragment was then mapped, resulting in a restriction map of pTPL2A. Southern analysis, using oligo 850, mapped the start of the *tpl* coding region to the 2.8-kbp *Eco*RV–*Pst*I fragment. We therefore subcloned this fragment into pBlueScript KS$^+$ to create pJL1. The exact position and orientation of the start of *tpl* within this fragment were determined using the polymerase chain reaction (PCR) with oligo 850 together with either of two primers that bind to plasmid sequences on opposite sides of the insert. The combination of oligo 850 and the M13 reverse sequencing primer yielded a 400-bp product, whereas no product was obtained from reactions using oligo 850 together with the M13 forward sequencing primer (data not shown). These results indicated that the start of the coding region for TPL was approximately 400 bp upstream of the *Eco*RV site in pTPL2A and that transcription is toward the *Eco*RV site.

Sequencing the tpl gene on both strands was done using the dideoxy chain termination method (Sanger et al., 1977) and Sequenase (U.S. Biochemicals). In addition to the 2.8-kbp *Eco*RV–*Pst*I fragment in pJL1, we subcloned the 1.7-kbp *Eco*RV–*Sal*I (pJL2) and the 1.5-kbp *Pst*I–*Sal*I (pJL3) fragment into pBlueScript KS$^+$. The entire *tpl* gene was then sequenced using primers that bound to the plasmid or custom primers within the gene.

Isolation and Sequencing of the Active Site Peptide. To a 2-mL solution of the holoenzyme (2.5 mg, 50 nmol of monomeric subunit) in 0.05 M Hepes–HCl buffer, pH 7.5, containing 20 μM EDTA and 0.20 mM DTT was gradually

Table II: Course of the Phase Modification by Means of Combination of the Phases from the Partial Model with MIR Phases

phase set	iso	comb-1	comb-2
R-factor of refined model (%)		27.6	24.0
resolution (Å)		2.7	2.5
rms bond distance (Å)		0.130	0.063
model completeness (%)		85	92
figure of merit at 2.7 Å	0.66	0.82	0.85
$\langle\Phi_{iso} - \Phi_{comb}\rangle$ (deg)		39	41

added a solution of NaB^3H_4 (140 mCi, 0.95 mg/mL) in dimethylformamide by aliquots of 20 μL in the dark under stirring. After the addition of 100 μL of the NaB^3H_4 solution, the activity of the solution decreased to 12% of that of the holoenzyme, and the solution exhibited the characteristic absorption band of a pyridoxamine at 325 nm. The reduced protein was dialyzed against 10 μM HCl and lyophilized.

Prior to BrCN cleavage of the protein, the free SH groups of the protein were alkylated by 4-vinylpyridine according to Friedman et al. (1970). Digestion of the protein by BrCN (50% w/w of monomeric subunit) was performed as described by Titani et al. (1972). The reaction mixture after dilution with water was lyophilized.

Purification of the peptide containing the phosphopyridoxyllysyl residue was performed by a combination of gel filtration and reverse-phase HPLC under various experimental conditions. The PTH derivative of N^{ϵ}-(phosphopyridoxyl)-lysine was identified by its radioactivity. Sequence determination was performed with a gas-phase sequencer, model 475 A (Applied Biosystems, Foster City, CA). A model 120 A PTH analyzer (Applied Biosystems) was used for on-line PTH detection. The amount of radioactivity released by each cycle of the sequence was determined. The 16 steps of the degradation were clearly identifiable except the fourth stage, which produced the most radioactivity. This step, which did not show an identifiable peak on the sequencer, was presumably the cofactor-labeled lysine residue.

Crystallization. Crystals of *C. intermedius* TPL apoenzyme were obtained with ammonium sulfate as precipitant under conditions reported earlier (Demidkina et al., 1988). Vapor diffusion with a pH gradient between the protein drop (pH 7.0) and reservoir (pH 6.0) yielded the best crystals. Before data collection, crystals were kept in a stabilizing solution containing 0.1 M MES–KOH (pH 6.0) with 1 M magnesium sulfate.

X-ray Data Collection. The space group is $P2_12_12$ with a = 76.0 Å, b = 138.3 Å, and c = 93.5 Å. There are two subunits of the tetrameric molecule in the asymmetric unit. Diffraction data for the native enzyme were collected by the rotation method (Arndt & Wonacott, 1977) using synchrotron radiation and an image plate scanner (J. Hendrix and A. Lentfer, unpublished results) as detector on the EMBL X11 beam line at the DORIS storage ring, DESY, Hamburg. Hard X-rays with a wavelength of 0.96 Å allowed the measurement of 173 366 reflections in the resolution range 2.3–15.0 Å using a single crystal (approximate size 1.0 × 0.7 × 1.0 mm). These were reduced to 43 435 unique reflections. The data are 97.8% complete to 2.3-Å resolution. The value of the merging R-factor ($R_I = \Sigma|I - \langle I\rangle|/\Sigma I$, where I is the intensity of reflection) was 5.8%. Main characteristics of the data set are given in Table I.

Table III: Statistics of the Refined Model

R-factor (%)	16.22
resolution (Å)	10.0–2.30
no. of reflections	43205
no. of atoms	7192
bond distances (Å)	
1–2 neighbors	0.012 (0.020)[a]
1–3 neighbors	0.038 (0.040)
1–4 neighbors	0.049 (0.050)
planar groups (Å)	0.012 (0.020)
chiral volumes (Å^3)	0.213 (0.200)
nonbonded contacts (Å)	
single torsion contacts	0.218 (0.500)
multiple torsion contacts	0.274 (0.500)
torsion angles (deg)	
planar	2.36 (5.0)
staggered	21.98 (15.00)
orthonormal	37.65 (30.00)
B-factor correlation (Å^2)	
main-chain bond	3.8 (4.0)
main-chain angle	5.8 (6.0)
side-chain bond	8.0 (8.0)
side-chain angle	10.3 (10.0)

[a] Root-mean-square deviations from the standard values are given with target values in parentheses.

Phase Modification and Structure Refinement. The starting model was a partial structure, 85% complete. The isomorphous phases with a figure of merit 0.66 in the resolution range 12.0–2.7 Å described in Antson et al. (1992) were also used. All computations were performed using the CCP4 program package (CCP4, 1979). Initial improvement of the electron density was achieved by combination of phases calculated from the partial atomic model with the isomorphous phases (Rice, 1981). Rebuilding of the atomic model was

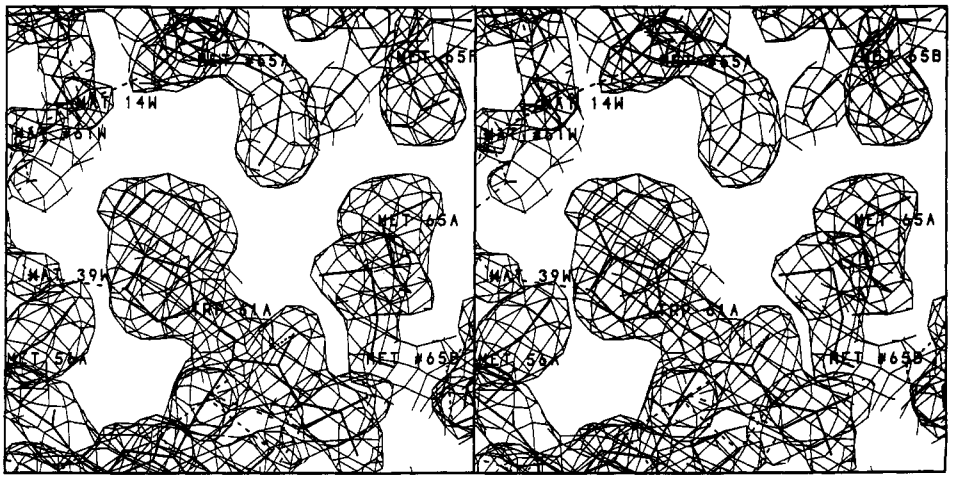

FIGURE 2: Stereo plot of the electron density for a part of the intersubunit hydrophobic cluster in the center of the molecule.

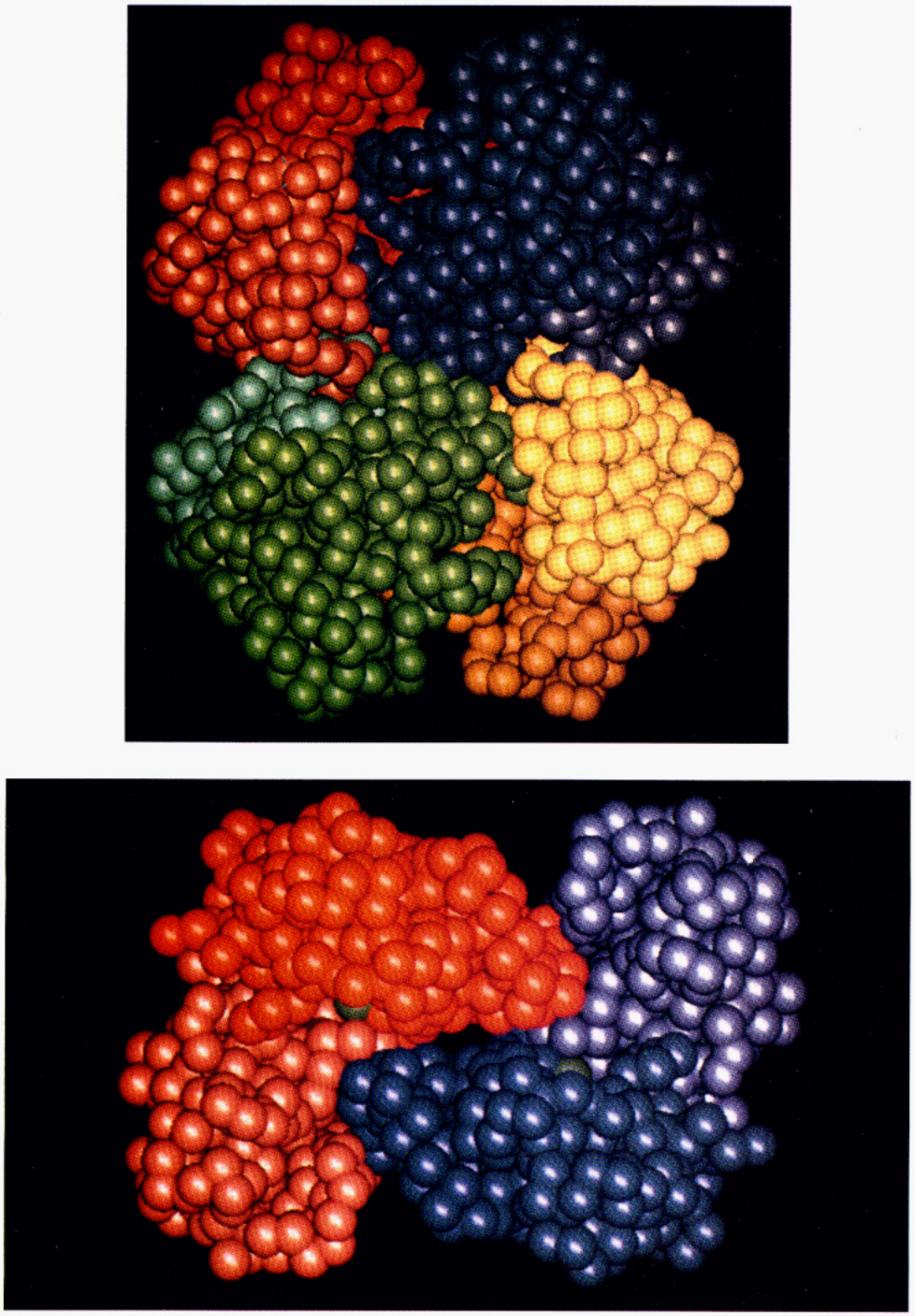

FIGURE 3: Space-filling model of TPL. Each residue is represented by a sphere of 3 Å drawn around the α-carbon. Subunits are shown in different colors with large domains in red, blue, green, and yellow. The color of the small domain is a variation in tone of the corresponding large domain color. (a, top) Tetramer viewed along the noncrystallographic axis of symmetry with the crystallographic 2-fold axis vertical. (b, bottom) View perpendicular to (a), from the top of the molecule toward the center. For clarity, only the dimer is shown. Spheres which correspond to the pyridoxal-P binding Lys257 are colored in green.

performed with the program FRODO (Jones, 1985) running on an Evans and Sutherland ESV series workstation using maps based on combined amplitudes (Stuart & Artymiuk, 1985) and combined phases (Bricogne, 1976; Hendrickson & Lattman, 1970). For the refinement of the model, restrained least-squares minimization (Hendrickson & Konnert, 1980) was used. The refinement was performed with individual isotropic temperature factors without the use of noncrystallographic symmetry restraints. After the second cycle of phase combination the figure of merit of the combined phases was 0.85 at 2.7-Å resolution, and the R-factor for the model to 2.5-Å resolution was 24.0% (Table II).

At this stage the model was sufficiently good to use the more usual Fourier synthesis based on coefficients $(2|F_o| - |F_c|) \exp(i\alpha_c)$ for manual rebuilding sessions. Rebuilding was performed independently for each crystallographically independent subunit. A further five rounds of refinement resulted in a model with an R-factor of 19.9% and an rms deviation between ideal and observed (1–2) bond distances of 0.017 Å. After inclusion of 450 water molecules per asymmetric unit the R-factor dropped to 17.6%. A further few rounds of refinement gave a model with an R-factor of 16.2% (statistics are given in Table III). In Figure 2, a representative section of electron density is shown for the $2|F_o| - |F_c|$ amplitudes and

phases from the current model. The coordinates have been deposited with the Brookhaven Protein Data Bank.

For structure comparison, the chicken mitochondrial AspAT coordinates kindly provided by J. Jansonius were used. The AspAT molecule was overlapped with the TPL dimer. Only the main-chain atoms of the βA, βG, βF, βE, and βD strands of the large domain β-sheet of one subunit were used for fitting of the overall molecule, giving an rms deviation of 0.94 Å. Analysis and interpretation of the structure of TPL was performed using the program O (Jones et al., 1991).

RESULTS

Cloning and Sequencing of Tyrosine Phenol-lyase. Figure 1 shows the nucleotide sequence of a 2100-bp region, including the complete *tpl* gene. This sequence has been deposited in the GenBank data base. A single open reading frame codes for a 456 amino acid polypeptide. The amino acid sequence of *E. coli* TRPase (Deeley & Yanofsky, 1981) is aligned with that of TPL in Figure 5. There is striking sequence homology between these two enzymes, with 43% of the residues being identical.

TPL is induced by L-tyrosine in *Erwinia herbicola* (Enei et al., 1973), *C. intermedius* (Kumagai et al., 1970a; Demidkina et al., 1984), and *C. freundii* (Carman & Levin, 1977). In *E. coli*, expression of TRPase is induced by L-tryptophan (Bilezikian et al., 1967; Stewart & Yanofsky, 1985). Translation of a leader peptide, *tna*C, is required for induction of TRPase in *E. coli* (Stewart & Yanofsky, 1986; Gollnick & Yanofsky, 1990). We examined the DNA sequence upstream of the start of *tpl*; however, we found no evidence for a potential leader peptide. This finding suggests that the mechanism of regulation of TPL expression in *C. freundii* is distinct from that controlling TRPase expression in *E. coli*.

Sequence of the Active Site Peptide. The sequence of the homogeneous radioactive peptide with characteristic fluorescence was SGKXDCLVNIAGGFLC, where X is the step which produced the most radioactivity. Alignment of the sequence of that peptide with the primary structure of TPL deduced from the gene structure (Figure 1) indicates that the lysine residue which binds PLP is K257. In the course of isolation of the active site peptide from the BrCN digest of the NaB^3H_4 reduced holoenzyme, four peptides were also isolated and purified to homogeneity. They were subjected to Edman degradation, and the sequences obtained are in agreement with corresponding parts of the TPL sequence deduced from the gene structure (Figure 1).

Crystal Structure. A space-filling representation of TPL is shown in Figure 3a. The large domains of all four subunits form a butterfly-like structure in which one pair of wings is rotated around the body by about 90° relative to the other. Small domains surround the central body of the butterfly and restrict possible movement of large domains. The tetramer has dimensions of about 80 × 60 × 105 Å. Two crystallographically related subunits form a dimer, as can be seen in Figure 3b. Two such dimers are related by noncrystallographic axes in the tetramer of TPL. The PLP-binding lysine residue (K257) is located in a cleft formed by residues from the large and small domains of one subunit and the large domain of a crystallographically related subunit. The distance between two NZ(K257) atoms of these two subunits is 26 Å.

The main-chain conformational (Φ,Ψ) angles are clustered in the allowed regions of the Ramachandran plot (Ramachandran & Sasisekharan, 1968), shown in Figure 4.

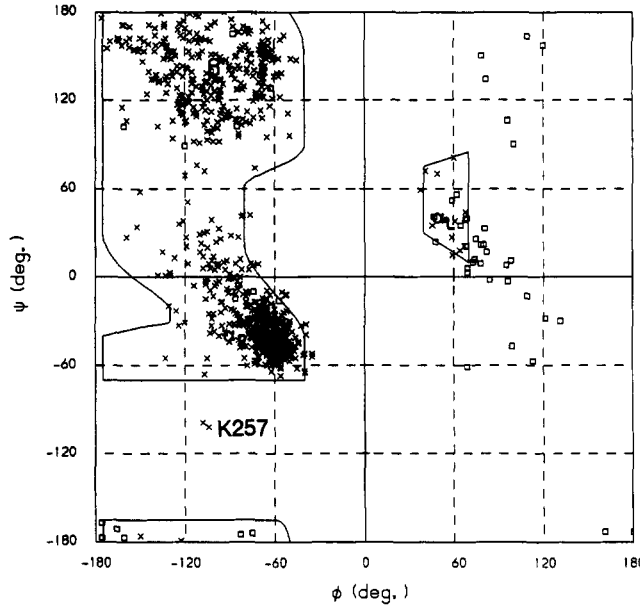

FIGURE 4: Ramachandran (Φ/Ψ) plot for two noncrystallographically related subunits. Squares mark glycine and crosses all other residues.

However, K257 lies outside the allowed regions. About 6% of the amino acids have poor electron density, probably due to high mobility in the absence of cofactor. These residues lie in three loops on the surface of the molecule: residues 123–131, 384–398, and 442–447 in one subunit and residues 123–133, 384–398, and 442–445 in that related by noncrystallographic symmetry.

The assignment of secondary structure to the amino acid sequence is given in Figure 5. About 34% of the amino acids are in α-helices, 17% in β-strands, and 16% in β-turns. A few regions of β-turns contain 3_{10} helices. One of these, residues 39–43, was previously, on the basis of the preliminary model, classified as α-helix 2 in Antson et al. (1992). The numbering of the secondary structure elements has been revised, and the structure is here described in new designations.

The sequence of α-helices and β-strands shows that TPL belongs to the α/β class of proteins (Levitt & Chothia, 1976). Each subunit can be divided into four parts: (1) the N-terminal arms, (2) the small domain, (3) the large domain, and (4) the connecting region between domains.

The small domain includes amino acids 19–48 and 333–456 (34% of the total). A four-stranded antiparallel β-sheet, shown in Figure 6a, forms the heart of the domain. All strands of the β-sheet (labeled in Figure 5 as βA′, βB′, βC′, βD′) are located in the C-terminal part of the small domain. The topology of the β-sheet in Richardson's notation (Richardson, 1977) is +1,+2*x*,−1, with the crossover being right-handed. The four α-helices of the small domain lie on the solvent-accessible side of the sheet. The N-terminal part of the domain is connected with the C-terminal by residues 45–47 which form a parallel β-bridge, βI, with strand βC′ and make an additional H-bond with the βD′ strand. Two C-terminal pieces of chain (436–440 and 452–456) make an antiparallel two-stranded β-ribbon, βII.

The large domain comprises residues 57–310 (56% of the total) and contains a seven-stranded β-sheet, shown in Figure 6b, and nine α-helices. The topology of the β-sheet is +5*x*,+1*x*,−2*x*,−1*x*,−1*x*,−1 in Richardson's notation, typical for aminotransferases. The strands of the β-sheet are marked βA, βG, βF, βE, βD, βB, and βC in Figure 5. These have directions (+,−,+,+,+,+,+), with all crossovers being right-

```
                        βX              α1                        β I
                       SSSSSS       HHHHHHHHHHTTTTTTTTTTTTT SSS
TPL       1 M.NYP..AEPFRIKSVETVSMIPRDERLKKMQEAGYNTFLLNSKDIYIDL 47
Trpase    1 MENFKHLPEPFRIRVIEPVKRTTRAYREEAIIKSGMNPFLLDSEDVFIDL 50

                    βY   α2                  α3           βA
                   SSSHHHHHHH            HHHHHHHHHHHHHH   SSSSS
TPL      48 LTDSGTNAMSDKQWAGMMMGDEAYAGSENFYHLERTVQELFGFKHIVPTH 97
Trpase   51 LTDSGTGAVTQSMQAAMMRGDEAYSGSRSYYALAESVKNIFGYQYTIPTH 100

                 α4                      βB
           HHHHHHHHHHHH T           TTTSSS S                 SS
TPL      98 QGRGAENLLSQLAIK.........PGQYVA.GNMYFTTTRYHQEKNGAVF 137
Trpase  101 QGRGAEQIYIPVLIKKREQEKGLDRSKMVAFSNYFFTTQGGHSQINGCTV 150

                βC                        α5             βD
               SSS TTTTTT    TTTTTT  HHHHHHHHHH TTTTTSSSSSSS   TT
TPL     138 VDIVRDEAHDAGLNIAFKGDIDLKKLQKLIDEKGAENIAYICLAVTVNLA 187
Trpase  151 RNVYIKEAFDTGVRYDFKGNFDLEGLERGIEEVGPNNVPYIVATITSNSA 200

                      α6              βE          α7
               TT    HHHHHHHHHHHHHTT SSSSSSTTHHHHHHHHHHHTTTTTTT H
TPL     188 GGQPVSMANMRAVRELTAAHGIKVFYDATRCVENAYFIKEQEQGFENKSI 237
Trpase  201 GGQPVSLANLKAMYSIAKKYDIPVVMDSARFAENAYFIKQREAEYKDWTI 250

                   α8       βF                 βG              α9
               HHHHHHHTTT SSSSSSSTTTTT    SSSSSS  H    HHHHHHHHHHH
TPL     238 AEIVHEMFSYADGCTMSGKKDCLVNIGGFLCMNDD...EMFSSAKELVVV 284
Trpase  251 EQITRETYKYADMLAMSAKKDAMVPMGGLLCMKDDSFFDVYTECRTLCVV 300

                            α10                    α11
               HH          HHHHHHHHHHHHHHHH HHHHHHHHHHHHHHHHHHHTT
TPL     285 YEGMPSYGGLAGRDMEAMAIGLREAMQYEYIEHRVKQVRYLGDKLKAAGV 334
Trpase  301 QEGFPTYGGLEGGAMERLAVGLYDGMNLDWLAYRIAQVQYLVDGLEEIGV 350

               βA'       βB'   α12             α13           βC'
               SSS      SSSSSSHHHHTTTT      HHHHHHHHHHHHHSSSSSSS
TPL     335 PIVEPVGGHAVFLDARRFCEHLTQDEFPAQSLAASIYVETGVRSMERGII 384
Trpase  351 .VCQQAGGHAAFVDAGKLLPHIPADQFPATGLACELYKVAGIRAVEIGSF 399

                                 βD'              α14
                               SSSSSSTTTT  HHHHHHHHHHHHHHHHTTTTTT
TPL     385 SAGRNNVTGEHHRPKLETVRLTIPRRVYTYAHMDVVADGIIKLYQHKEDI 434
Trpase  400 LLGRDPKTGKQLPCPAELLRLTIPRATYTQTHMDFIIEAFKHVKENAANI 449

                 βII             βII
                SSSSS           SSSSS
TPL     435 RGLKFIYEPKQLRFFTARFDYI 456
Trpase  450 KGLTFTYEPKVLRHFTAKLKEV 471
```

FIGURE 5: Sequence of TPL with assignment of secondary structure. Residues which belong to α-helices, β-strands, and β-turns are outlined by the letters H, S, and T, respectively. Designations of helices and strands are shown in a separate line. The sequence of *E. coli* TRPase [from Deeley and Yanofsky (1981)] is overlaid for comparison.

handed. Helices $\alpha 2$, $\alpha 3$, $\alpha 5$, $\alpha 6$, $\alpha 7$, $\alpha 8$, and $\alpha 10$ are situated on one side of the β-sheet and shield it from solvent. Helices $\alpha 4$ and $\alpha 9$ are situated on the opposite, interdomain interface side of the sheet.

The connecting region between the domains is formed by residues 49–56 and 311–332. It includes helix $\alpha 11$, which is about 35 Å long and contains 20 amino acids. In contrast to the structure of AspAT (Jansonius & Vincent, 1987), there is no kink apparent in the helix. Nevertheless, the ends of the helix are at an angle of about 25° to one other. The first connecting piece of the chain lies in the cavity between two domains. Helix $\alpha 11$ lies on the surface of the subunit.

Intersubunit Contacts. A schematic representation of the molecular architecture is shown in Figure 7 with the crystallographic symmetry axis vertical. The overall symmetry of the molecule is 222. The tetrameric α_4 molecule of TPL is to be considered from a strictly crystallographic point of view as $\alpha_2\alpha'_2$, where the α and α' subunits are related by noncrystallographic 2-fold axes. The two α subunits are related by a crystallographic 2-fold axis marked Q, as are the two α' subunits. These pairs of crystallographically related subunits are from now on referred to as dimers. The contact between subunits in the dimer includes two active sites and is discussed further in the next section. The two dimers are related by the noncrystallographic symmetry axes P and R. Intersubunit contacts between dimers include the N-terminal arms and the hydrophobic cluster at the center of the molecule. The N-terminal arms (residues 1–18) of two subunits related by the molecular axis R intertwine and form an antiparallel β-structure in the contact region. The position of the subunits relative to that contact is stabilized by two other β-strands, formed by amino acids 56–58. Each of these strands is connected with the N-terminal strand of an adjacent subunit, being parallel to it. The resulting four-stranded β-sheet, Figure 6c, is made up of two pairs of adjacent parallel strands, the two pairs being antiparallel to one other. Strands of that β-sheet are marked as βX and βY in Figure 5. Residue 11, which resides in the middle of the βX strand, has conformational angles which are typical for α-helices. That makes a kink in the βX strand and allows two such strands from

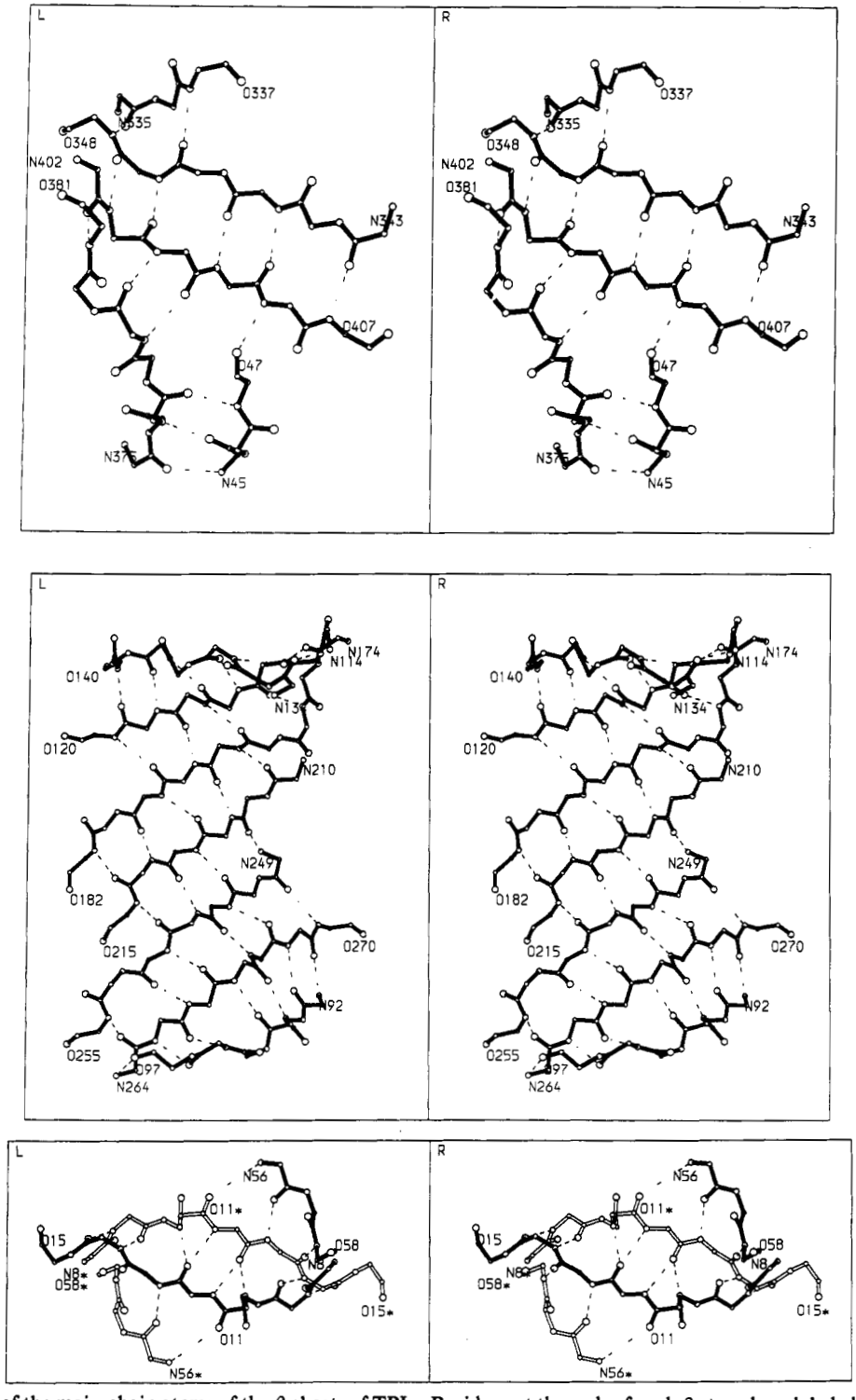

FIGURE 6: Stereo plot of the main-chain atoms of the β-sheets of TPL. Residues at the ends of each β-strand are labeled. H-Bonds are shown by dashed lines. (a, top) Four-stranded β-sheet of the small domain, as seen from the large domain. The order of strands from top to bottom is βA′, βB′, βD′, and βC′. Residues 45–47 which form the β-bridge βI are also shown. (b, middle) β-Sheet in the large domain, as seen from the small domain. The order of strands from top to bottom is βC, βB, βD, βE, βF, βG, and βA. (c, bottom) Intersubunit β-sheet, viewed along the 2-fold crystallographic axis. Lower subunit β-strands are shown by open bonds and upper subunit β-strands by filled bonds. The oxygen of residue 11, which is in an α-helical conformation, is marked.

adjacent subunits to intertwine. The N-termini are anchored on helix α11 from their "own" subunit, making an H-bond between the OH group of Y3 and the OD2 atom of D327.

In the center of the molecule there is an interesting hydrophobic cluster, shown in Figure 8. It includes residues M56, M64, M65, and W61 from each of the four subunits, comprising 4 Trp and 12 Met residues. Three of these amino acids, W61, M64, and M65, are located on helix α2. The core of the cluster is made up of the four M65 residues, the sulfur atoms of which lie at the corners of a tetrahedron with edges of about 5 Å. The next shell of the cluster is composed of the four W61 indole rings. In front and behind of the view in Figure 8 the hydrophobic core is surrounded by four helices α2 which are generally parallel to the axis marked R in Figure 7. The top and bottom of the hydrophobic cluster are formed by M56 residues.

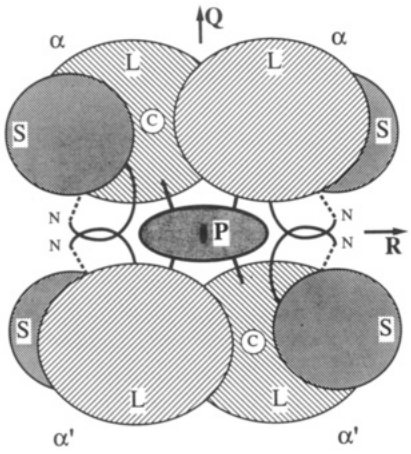

FIGURE 7: Schematic representation of the domain architecture and intersubunit contacts in TPL. The view is the same as in Figure 3a, with the crystallographic 2-fold axis (Q) vertical and one of the noncrystallographic axes (R) horizontal. Pairs of crystallographically related subunits are marked as α and α'. Large domains are marked as L and small domains as S, the catalytic cleft is marked as C, and N-termini are marked as N.

Active Site. We were not able to obtain well-ordered crystals of the holoenzyme either by holoenzyme crystallization or by soaking the apoenzyme crystals in PLP-containing solutions. However, the location of the PLP-binding lysine (K257) and the presence of a strong electron density feature close to it, which we ascribe to a free sulfate group, show where PLP is likely to be located in the holoenzyme. As in the structures of the several aminotransferases [full references are given in Fukui et al. (1991)], the PLP-binding lysine lies in the short loop between the βF and βG strands of the large domain β-sheet. The active site cavity (Figure 9) is formed by residues T49, D50, S51, and G52 from the connecting region; Q98, G99, R100, N185, D214, A215, T216, R217, S254, G255, K256, and K257 from the large domain; H343 and R404 from the small domain; and Y71 and E286 from the large domain of the crystallographically related subunit. The sulfate ion, which is likely to be replaced by the phosphate group of PLP in the holoenzyme, makes a number of H-bonds with residues in the active site cleft. H-Bonds are formed between atoms: O1 and N(G99), O1 and OG(S254), O2 and N(R100), O3 and NE2(Q98), and O4 and NZ(K257). The distance between the sulfur atom of sulfate and NZ(K257) is about 4.2 Å.

DISCUSSION

It has been proposed that the stereochemistry of the cofactor protonation of PLP-dependent enzymes provides evidence for the evolution of this entire family of enzymes from a common progenitor (Dunathan & Voet, 1974). Thus, it could be suggested that at least the fold of the PLP-binding domain is repeated in all PLP-dependent enzymes involved in amino acid metabolism, just as the dinucleotide-binding domain fold is repeated in the NAD-dependent dehydrogenases (Rossmann et al., 1974). However, in the case of the vitamin B_6-dependent enzymes, two types of fold for the PLP-binding domains have been found. The polypeptide chain fold and subunit architecture in the β_2-dimer of the $\alpha_2\beta_2$ molecule of tryptophan synthase (Hyde et al., 1988) are quite different from those found in the aminotransferases (Ford et al., 1980).

The sequence alignment of TPL to different AspAT does not reveal significant sequence homology (23% identity in the case of *E. coli* AspAT). However, it appears that the folding of the PLP-binding domain of TPL is similar to that of AspAT, as shown in Figure 10. The small domains of these proteins are not very similar to one other. Nevertheless, one motif in the β-structure topology of the small domain of AspAT, where the N-terminal part is connected with the C-terminal by formation of main-chain H-bonds with two chains of the C-terminal β-sheet (Jansonius & Vincent, 1987), is repeated in TPL (Figure 6a). A difference is that the β-sheet contains three strands in AspAT, while in TPL there are four strands. The structures of the active sites of both proteins have certain similarities. Not surprisingly, most of the residues of AspAT which bind PLP (Kirsch et al., 1984) are conserved in TPL, as shown in Figure 11. Residues K258, D222, and N194 of AspAT which bind the pyridoxal moiety correspond to residues K257, D214, and N185 in the three-dimensional structure of TPL; residues Y70, G108, and S255 (phosphate-binding site) correspond to Y71, G99, and S254. The main-chain atoms of T109 in AspAT, whose N atom H-bonds to one of the phosphate oxygens, coincide with those of R100 in TPL. Y71 of TPL is placed somewhat further from the active site than the corresponding residue in AspAT, probably because the apo form of TPL is being compared with the holo form of AspAT. These similarities in polypeptide chain folding and in cofactor binding sites suggest that TPL evolved from a common node in an evolutionary tree to the aminotransferases.

Another representative of the family of β-eliminating lyases, TRPase, the three-dimensional structure of which is not yet known, has substantial sequence homology with TPL (Figure 5) (43% identity in the case of *E. coli* TRPase). All residues suggested above to be responsible for the binding of PLP in TPL are conserved in the sequence of TRPase. The active site lysine of TPL was identified at position K257 (labeled with an asterisk in Figure 1) by reduction with $NaBH_4$, cyanogen bromide cleavage, isolation of the labeled peptide, and Edman sequencing. In TRPase, the active site lysine is K270 (Kagamiyama et al., 1972), and it is preceded by another lysine, K269. We have found that replacement of K269 by arginine in TRPase results in a significant reduction of activity (Phillips et al., 1991). Thus, it is interesting that K257 in TPL, which binds PLP, is also preceded by a lysine, K256. On the basis of the data of Kumagai et al. (1975) and Faleev et al. (1988), the α-proton abstraction in TPL may be performed by a histidine residue. We believe that H343 may be this catalytic base, which was shown to exhibit a pK_a of 7.6 (Kiick & Phillips, 1988a). In TRPase, the corresponding H358 is located in a highly conserved region of the sequence.

From the comparison of the three-dimensional structures of AspAT and TPL, it appears that two arginine residues of TPL, R381 and R404, are closest to the position of the R386 of AspAT (Figure 11), the guanidinium group of which binds the α-carboxylate group of the substrate (Kirsch et al., 1984). One of these arginines, R404, is conserved in the structure of TRPase (Figure 5). R404 resides on the N-terminal end of the βD′ strand of the small domain β-sheet, similar to the part in which R386 is located in the structure of AspAT (Jansonius & Vincent, 1987). Thus, we postulate that R404 is responsible for the α-carboxylate binding.

The chemical mechanisms of TPL and TRPase are very similar (Kiick & Phillips, 1988a,b). The substrate specificity should be controlled by the interactions of the phenol or indole side chain with a second catalytic base within a hydrophobic pocket. Thus, the substrate selectivity is controlled during the β-elimination step rather than at the stage of substrate binding (Faleev et al., 1988). Identification of the substrate binding pocket will require studies of a stable amino acid complex.

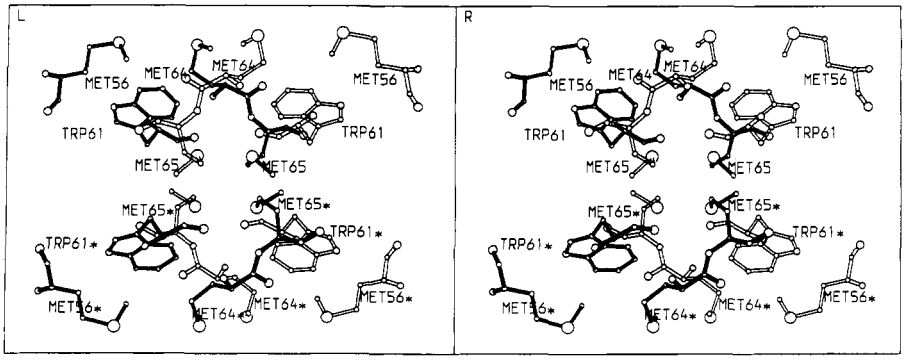

FIGURE 8: Stereo plot of the hydrophobic cluster in the same view as in Figure 7. Residues from one subunit of the dimer are shown by filled bonds and residues from the other by open bonds. Residues related by noncrystallographic symmetry are indicated by an asterisk.

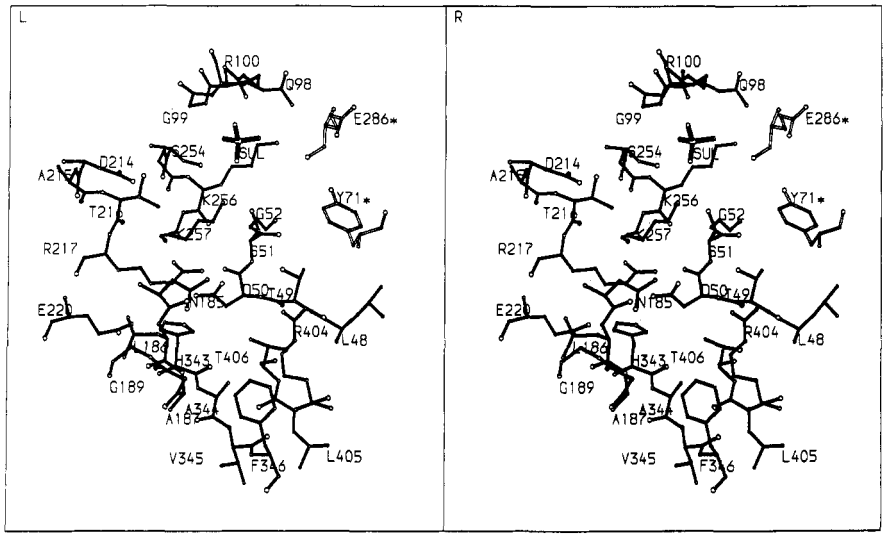

FIGURE 9: Structure of the catalytic cleft. Residues from one subunit are shown by filled bonds while residues from the crystallographically related subunit are shown by open bonds and indicated by an asterisk. The sulfate ion is shown by thicker filled bonds.

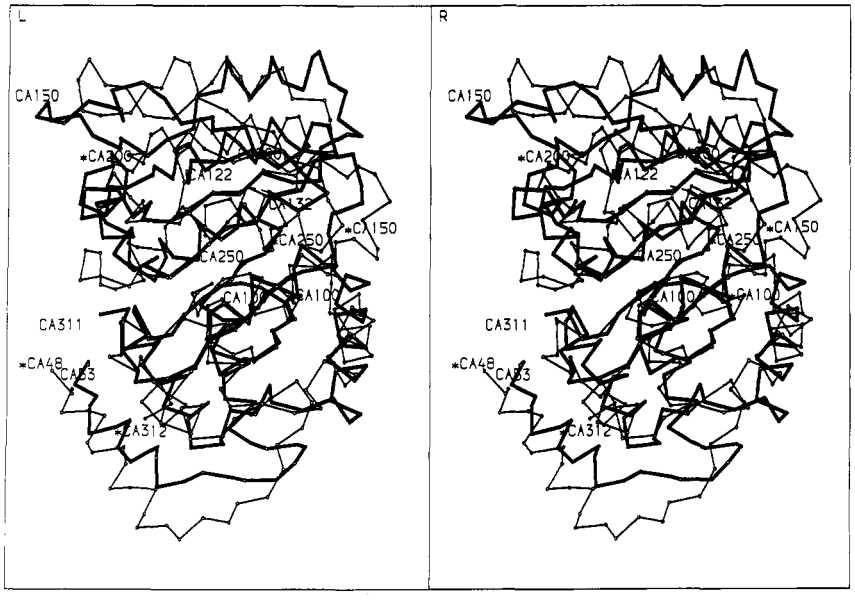

FIGURE 10: Superimposed C_α backbones of the large domains of TPL (thick lines) and chicken mitochondrial AspAT (thin lines). Some of the C_α atoms of TPL and of AspAT (indicated by an asterisk) are marked.

After our work on the sequence determination was completed, the amino acid sequences of TPL from *C. intermedius* and *C. freundii* were independently deduced (Iwamori et al., 1991; Kurusu et al., 1991). Although the DNA sequences of our gene and these genes differ at 15 positions, the deduced amino acid sequences are identical. In this regard, it is interesting that we have observed several differences in the kinetic behavior of TPL isolated from the two bacteria. For example, the K_m for *S*-(*o*-nitrophenyl)-L-cysteine is 5-fold higher for TPL from *C. intermedius* (0.5 mM) than that of the *C. freundii* enzyme (0.1 mM) (N. Faleev and R. Phillips, unpublished results).

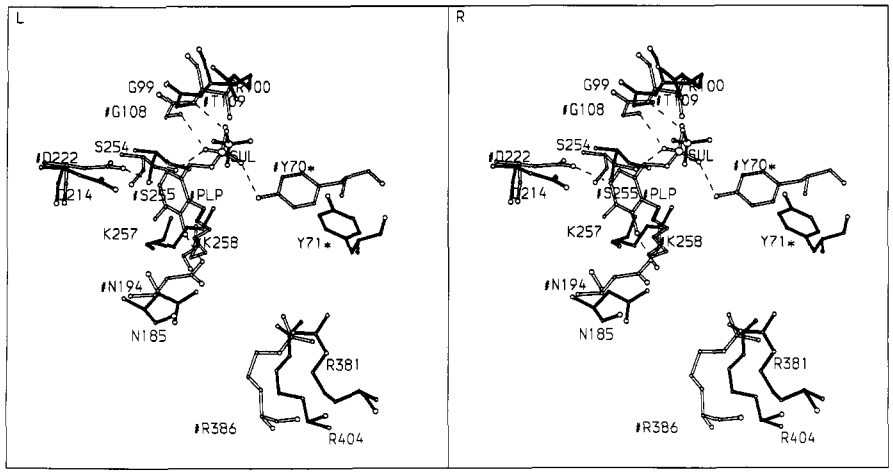

FIGURE 11: Superposition of the PLP and α-carboxylate binding residues of AspAT (open bonds) with corresponding TPL residues (filled bonds). For AspAT, PLP, and TPL, the sulfates are also shown.

From the comparison of the domain architecture of TPL and AspAT, it follows that the mutual arrangement of domains in each of the two "dimers" of TPL (each including a crystallographic 2-fold axis) is similar to that in the dimeric molecule of AspAT. The TPL dimers are bound through the hydrophobic cluster in the center of the molecule and by two pairs of intertwined N-terminal arms. In fact, the hydrophobic cluster binds together the large domains of all four subunits. The N-terminal arms bind the small domains of noncrystallographically related subunits; such intersubunit contact through β-sheets has been previously observed in the three-dimensional structures of retroviral aspartic proteinases [see, e.g., Wlodawer et al. (1989)]. There, the interpenetration of subunits through the common β-sheet results in the formation of a stable dimer and is essential for catalysis (Rao et al., 1991). The mutual connection of the large and small domains of the noncrystallographically related subunits of TPL through the interdimer interface suggests that conformational changes in one dimer might affect the conformation of the related dimer and thus influence the catalytic properties of the enzyme.

The results reported herein lay the groundwork for future investigations on the structure of TPL, including the study of the mechanism of action by inhibitor binding and site-directed mutagenesis.

ACKNOWLEDGMENT

We thank J. Jansonius for providing us with the coordinates of the AspAT and for helpful discussions. We are grateful to N. Bazulina for kind help with fluorescence measurements. We also thank C. Yanofsky for assistance in the cloning of TPL, which was performed in his laboratory at Stanford University.

REFERENCES

Antson, A. A., Strokopytov, B. V., Murshudov, G. N., Isupov, M. N., Harutyunyan, E. H., Demidkina, T. V., Vassylyev, D. G., Dauter, Z., Terry, H., & Wilson, K. S. (1992) *FEBS Lett. 302*, 256–260.

Arndt, U. W., & Wonacott, A. J., Eds. (1977) *The Rotation method in crystallography*, Elsevier, Amsterdam and New York.

Arnone, A., Rogers, P. H., Hyde, C. C., Briley, P. D., Metzler, C. M., & Metzler, D. E. (1985) in *Transaminases* (Christen, P., & Metzler, D. E., Eds.) pp 138–155, J. Wiley and Sons, New York.

Benton, W. D., & Davis, R. W. (1977) *Science 196*, 180–182.

Bilezikian, J., Kaimpfer, R., & Magasanik, B. (1967) *J. Mol. Biol. 27*, 495–506.

Borisov, V. V., Borisova, S. N., Sosfenov, N. I., & Vainshtein, B. K. (1980) *Nature 284*, 189–190.

Bricogne, G. (1976) *Acta Crystallogr. A32*, 832–847.

Carman, G. M., & Levin, R. E. (1977) *Appl. Environ. Microbiol. 33*, 192–198.

CCP4 (1979) *The SERC (U.K.) Collaborative Computing Project No. 4: a Suite of Programs for Protein Crystallography*, Daresbury Laboratory, Warrington, England.

Deeley, M. C., & Yanofsky, C. (1981) *J. Bacteriol. 147*, 787–796.

Demidkina, T. V., Myagkikh, I. V., Faleev, N. G., & Belikov, V. M. (1984) *Biokhimiya (Engl. Transl.)*, 27–31.

Demidkina, T. V., Myagkikh, I. V., Antson, A. A., & Harutyunyan E. H. (1988) *FEBS Lett. 232*, 381–382.

Duffey, S. S., & Blum, M. S. (1977) *Insect. Biochem. 7*, 57–65.

Duffey, S. S., Aldrich, J. R., & Blum, M. S. (1977) *Comp. Biochem. Physiol. 56B*, 101–102.

Dunathan, H. C., & Voet, J. G. (1974) *Proc. Natl. Acad. Sci. U.S.A. 71*, 3888–3891.

Enei, H., Matsui, H., Yamashita, K., Okumura, S., & Yamada, H. (1972) *Agric. Biol. Chem. 36*, 1861–1868.

Enei, H., Yamashita, K., Okumura, S., & Yamada, H. (1973) *Agric. Biol. Chem. 37*, 485–492.

Faleev, N. G., Ruvinov, S. B., Demidkina, T. V., Myagkikh, I. V., Gololobov, M. Y., Bakhmutov, V. I., & Belikov, V. M. (1988) *Eur. J. Biochem. 177*, 395–401.

Ford, G. C., Eichele, G., & Jansonius, J. N. (1980) *Proc. Natl. Acad. Sci. U.S.A. 77*, 2559–2563.

Friedman, M., Krull, L., & Cavins, J. F. (1970) *J. Biol. Chem. 245*, 3868–3871.

Fukui, T., Kagamiyama, H., Soda, K., & Wada, H., Eds. (1991) *Enzymes Dependent on Pyridoxal Phosphate and Other Carbonyl Compounds as Cofactors*, Part II, Pergamon Press, Oxford.

Gollnick, P., & Yanofsky, C. (1990) *J. Bacteriol. 172*, 3100–3107.

Harutyunyan, E. G., Malashkevich, V. N., Tersyan, S. S., Kochkina, V. M., Torchinsky, Yu. M., & Braunstein, A. E. (1982) *FEBS Lett. 138*, 113–116.

Hendrickson, W. A., & Konnert, J. H. (1980) in *Computing in Crystallography* (Diamond, R., Ramaseshan, S., & Venkatesan, K., Eds.) pp 13.01–13.25, Indian Academy of Sciences, Bangalore, India.

Hendrickson, W. A., & Lattman, E. E. (1970) *Acta Crystallogr. B26*, 136–143.

Hyde, C. C., Ahmed, S. A., Padlan, E. A., Miles, E. W., & Davies, D. R. (1988) *J. Biol. Chem. 263*, 17857–17871.

Iwamori, S., Yoshino, S., Ishiwata, K. I., & Makiguchi, N. (1991) *J. Ferment. Bioeng. 72*, 147–151.

Jansonius, J. N., & Vincent, M. G. (1987) in *Biological Macromolecules and Assemblies* (Jurnak, F. A., & McPherson, A., Eds.) Vol. 3, pp 187–285, J. Wiley and Sons, New York.
Jones, A. (1985) *Methods Enzymol. 115*, 157–171.
Jones, T. A., Zou, J.-Y., Cowan, S. W., & Kjeldgaard, M. (1991) *Acta Crystallogr. A47*, 110–119.
Kagamiyama, H., Matsubara, H., & Snell, E. E. (1972) *J. Biol. Chem. 247*, 1576–1585.
Kawata, Y., Tani, S., Sato, M., Katsube, Y., & Tokushige, M. (1991) *FEBS Lett. 284*, 270–272.
Kazakov, V. K., Tarusina, I. I., Myagkikh, I. V., & Demidkina, T. V. (1987) *Biokhimiya (Moscow) 52*, 1319–1323.
Kiick, D. M., & Phillips, R. S. (1988a) *Biochemistry 27*, 7333–7338.
Kiick, D. M., & Phillips, R. S. (1988b) *Biochemistry 27*, 7339–7344.
Kirsch, J. F., Eichele, G., Ford, G. C., Vincent, M. G., & Jansonius, J. N. (1984) *J. Mol. Biol. 174*, 497–525.
Kondo, K., Wakabayashi, S., & Kagamiyama, H. (1987) *J. Biol. Chem. 262*, 8648–8659.
Kumagai, H., Yamada, H., Matsui, H., Ohkishi, H., & Ogata, K. (1970a) *J. Biol. Chem. 245*, 1767–1772.
Kumagai, H., Yamada, H., Matsui, H., Ohkishi, H., & Ogata, K. (1970b) *J. Biol. Chem. 245*, 1773–1777.
Kumagai, H., Utagawa, T., & Yamada, H. (1975) *J. Biol. Chem. 250*, 1661–1667.
Kurusu, Y., Fukushima, M., Kohama, K., Kobayashi, M., Terasawa, M., Kumagai, H., & Yukawa, H. (1991) *Biotechnol. Lett. 13*, 762–772.
Levitt, M., & Chothia, C. (1976) *Nature 261*, 552–557.
Phillips, R. S. (1987) *Arch. Biochem. Biophys. 256*, 302–310.
Phillips, R. S., Von Tersch, R. L., Miles, E. W., & Ahmad, S. A. (1987) *Biochemistry 26*, 4163 (Abstract).
Phillips, R. S., Richter, I., Gollnick, P., Brzovic, P., & Dunn, M. F. (1991) *J. Biol. Chem. 266*, 18642–18648.
Ramachandran, G. N., & Sasisekharan, V. (1968) *Adv. Protein Chem. 23*, 283–437.
Rao, J. K., Erickson, J. W., & Wlodawer, A. (1991) *Biochemistry 30*, 4663–4671.
Rice, D. W. (1981) *Acta Crystallogr. A37*, 491–500.
Richardson, J. C. (1977) *Nature 268*, 495–500.
Rossmann, M. G., Moras, D., & Olsen, K. W. (1974) *Nature 250*, 194–199.
Sambrook, J., Fritsch, E. F., & Maniatis, T. (1989) *Molecular Cloning, a Laboratory Manual*, Cold Spring Harbor Press, Cold Spring Harbor, NY.
Sanger, F. S., Niklen, S., & Coulsen, A. R. (1977) *Proc. Natl. Acad. Sci. U.S.A. 74*, 5463–5467.
Stewart, V., & Yanofsky, C. (1985) *J. Bacteriol. 164*, 731–740.
Stewart, V., & Yanofsky, C. (1986) *J. Bacteriol. 167*, 383–386.
Stuart, D. I., & Artymiuk, P. J. (1985) *Acta Crystallogr. A40*, 713–716.
Titani, K., Hermodson, M. A., Ericsson, L. H., Walsh, K. A., & Neurath, H. (1972) *Biochemistry 11*, 2427–2435.
Wlodawer, A., Miller, M., Jaskolski, M., Sathyanarayana, B. K., Baldwin, E. T., Weber, I. T., Selk, L. M., Clawson, L., Schneider, J., & Kent, S. B. H. (1989) *Science 245*, 616–621.